Chiroptical responses modulated by competitions between structural chiralities and magnetizations

Chunchao Wen, Jianfa Zhang,* Chaofan Zhang, Shiqiao Qin, Zhihong Zhu, and Wei Liu†

College for Advanced Interdisciplinary Studies, National University of Defense Technology, Changsha 410073, People's Republic of China and Nanhu Laser Laboratory and Hunan Provincial Key Laboratory of Novel Nano-Optoelectronic Information Materials and Devices, National University of Defense Technology, Changsha 410073, People's Republic of China

(Received 11 April 2024; accepted 17 May 2024; published 3 June 2024)

We study chiroptical scattering properties of magneto-optical structures possessing rotation symmetries, with both rotation axis and externally applied static magnetic field parallel to the incident direction. For no less than threefold rotation symmetries (with or without magnetizations), cross sections of scattering and extinction are invariant as long as the incident polarizations locate on the same latitude line of the Poincaré sphere (polarization ellipses of the same ellipticity but different orientations), while for general incident polarizations, cross sections of scattering and extinction are ellipticity-weighted arithmetic average of those for circularly polarized incident waves. We further characterize the chiroptical responses through relative distinctions between cross sections for incident waves of left-handed and right-handed circular polarizations, and reveal that the external magnetic field can both suppress and enhance the chiroptical responses, depending on its direction and strength. When the chiroptical response is fully eliminated by the magnetization, the cross sections get decoupled to the polarization ellipticities as well, becoming fully independent of arbitrary incident polarizations. Our arguments are based on global structural symmetries only, and thus all conclusions drawn are irrelevant to local geometric parameters or specific material parameters of the scatterers, as long as the rotation symmetry is preserved. The principles we have revealed can be applied in many magnetism-induced nonreciprocal structures, and are robust against any rotation-symmetry-preserving structural defects and perturbations.

DOI: 10.1103/PhysRevA.109.063502

I. INTRODUCTION

Studies of chiroptical responses induced by structural chiralities or nonreciprocal magnetizations both date back to the 19th century and currently constitute a main theme pervading most branches of photonics [1–4]. Early studies were largely concentrated on clusters (such as solutions) of chiral molecules that are abundant and randomly distributed, which are effectively isotropic as there is no preferred orientation direction. As a result, light incident at any direction effectively interacts with chiral molecules of all possible orientations, and the chiroptical responses obtained are thus automatically molecular orientation averaged, being naturally independent of the incident direction [1]. In recent years, with the rapid development of high-precision fabrication nanotechnology, a significant portion of investigations into optical chiralities is shifted from randomly distributed to highly oriented systems with different sorts of symmetries [2–4]. This has significantly broadened the horizons of chiral photonics and rendered enormous flexibilities for explorations of the interplay among structural orientations and geometric symmetry, electromagnetic duality symmetry, optically induced artificial magnetism, and magnetization that breaks reciprocity [1–12].

Here, we study the chiroptical responses of magneto-optical scattering particles that are no less than threefold rotationally symmetric. The optical chirality is characterized by relative distinctions between cross sections of extinction and scattering, for incident waves of right-handed and left-handed circular polarizations (RCP and LCP). When rotation symmetry axis, incident direction, and external static magnetic field are parallel, cross sections of extinction and scattering are correlated with ellipticities (positive and negative for left and right handedness, respectively) while irrelevant to orientations (in terms of semimajor axis) of the incident polarization ellipses. For general polarizations, cross sections are ellipticity-weighted arithmetic average of those for LCP and RCP incident waves. As a result, extinction and scattering cross sections always reach their extremes (maximum and minimum) for circularly polarized (CP) incident waves. We further show that magnetizations can enhance or suppress the chiroptical responses, depending on the direction and strength of the externally applied magnetic field. When the chiroptical response in terms of scattering (extinction) is fully eliminated, with or without external magnetizations, the scattering (extinction) cross sections would become fully independent of the polarization ellipticity too, remaining invariant for incident waves of arbitrary polarizations. Our reasoning is solely based on the symmetry arguments, and thus all conclusions drawn are irrelevant to local geometric or material parameters of the scatterers, as long as the rotation symmetry is preserved. Our study on chiroptical responses modulated by the interplay among geometric chiralities, rotation symmetries, and static magnetizations could play a significant role in both fundamental explorations

*jfzhang85@nudt.edu.cn
†wei.liu.pku@gmail.com

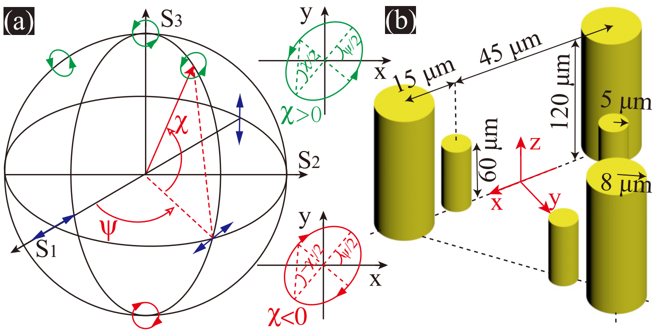

FIG. 1. (a) The Poincaré sphere (parametrized by three Stokes parameters $S_{1,2,3}$) employed to represent incident polarizations. The latitude χ corresponds to ellipticity of the polarization ellipse ($\chi > 0$ for left-handedness on the northern hemisphere; $\chi < 0$ for right-handedness on the southern hemisphere; $\chi = 0$ for linear polarizations) and longitude ψ corresponds to the ellipse orientation. (b) A scattering configuration consisting of six cylinders orientated along the z axis and made of magneto-optical materials (geometric parameters specified within the figure) that exhibits C_3 rotation symmetry (rotation axis along the z axis) and no mirror symmetry. Both the incident direction and the externally applied magnetic field are parallel to the rotation symmetry axis.

and practical applications relying on magnetism-induced nonreciprocity.

II. THEORETICAL MODEL AND FORMALISMS FOR SCATTERINGS AND CHIROPTICAL RESPONSES

The polarization of the incident wave can be represented through the Poincaré sphere [parametrized by the Stokes vector (S_1, S_2, S_3) or angle vector $(\chi,\ \psi)$, whose entries are, respectively, latitude and longitude as shown in Fig. 1(a)] [13,14]: $\chi \in [-\pi/2, \pi/2]$ characterizes the ellipticities of the polarization ellipses, with positive and negative χ (northern and southern hemisphere) corresponding to left- and right-handedness, respectively (see Fig. 1; LCP and RCP waves locate, respectively, at $S_3 = \pm 1$ and $\chi = \pm\pi/2$, and all linear polarizations locate on the great circle $S_3 = 0$ and $\chi = 0$); latitude $\psi \in [0, 2\pi]$ characterizes the orientations of the polarization ellipses in terms of the semimajor (or semiminor) axis (see Fig. 1; $\psi = 0$ and $\psi = \pi$ for semiaxis along x and y, respectively; the semiaxes for LCP and RCP waves are not defined, and so are ψ at $S_3 = \pm 1$). For an incident wave of polarization locating at (χ_i, ψ_i) on the Poincaré sphere, the unit field vector $\hat{\mathbf{E}}_i$ can be represented in CP unit basis ($\hat{\mathbf{R}}$ and $\hat{\mathbf{L}}$) as

$$\hat{\mathbf{E}}_i = \sin\left(\frac{\pi}{4} - \frac{\chi_i}{2}\right)\mathrm{e}^{\mathrm{i}\psi_i/2}\hat{\mathbf{R}} + \cos\left(\frac{\pi}{4} - \frac{\chi_i}{2}\right)\mathrm{e}^{-\mathrm{i}\psi_i/2}\,\hat{\mathbf{L}}. \quad (1)$$

Here, it is clear that the polarization is directly expressed in terms of half the Poincaré angles of $\chi/2$ and $\psi/2$ rather than the angles themselves. The underlying profound mathematics is that polarizations correspond to 1-spinors, which are effectively the square roots of the Stokes vectors [15,16].

When the whole scattering configuration exhibits n-fold ($n \geqslant 3$) rotation symmetry (both the incident direction and the external magnetic field are parallel to the rotation axis, which are fixed along the z direction), it has been previously proved that the two scattering channels of incident LCP and RCP waves are fully decoupled from each other [7]. That is, for unit-amplitude incident waves of arbitrary polarizations, the cross sections of scattering and extinction (C_{sca} and C_{ext})

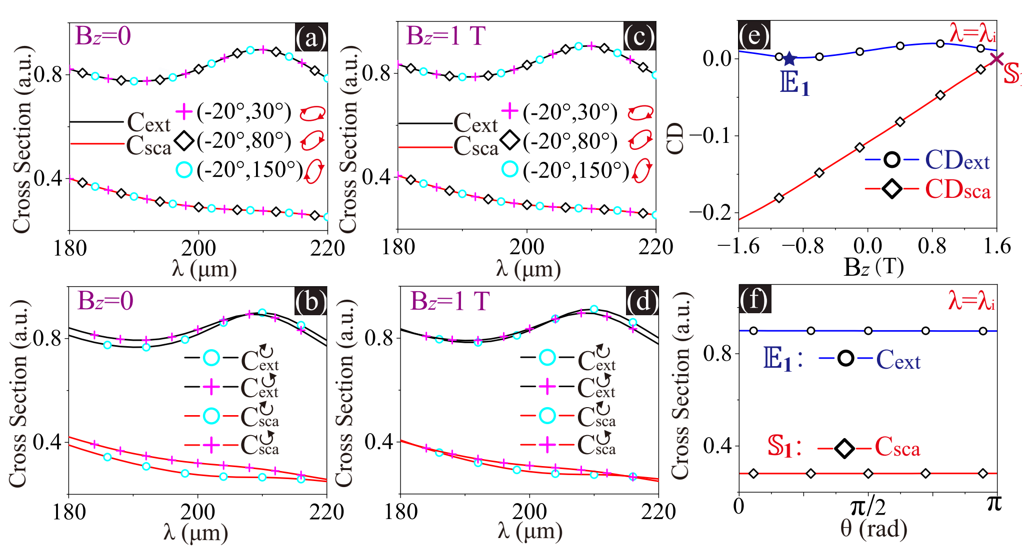

FIG. 2. Scattering and extinction spectra for incident polarizations on the same [(a) and (c); invariant χ; the corresponding angle vectors $(\chi,\ \phi)$ are specified] and different [(b) and (d); RCP and LCP] latitude lines, with zero [(a) and (b); $B_z = 0$] and nonzero [(c) and (d); $B_z = 1$ T] magnetizations. (e) The dependence of $\mathrm{CD}_{\mathrm{sca,ext}}$ on B_z at a randomly selected incident wavelength $\lambda_i = 210$ μm. Two points ($\mathbb{E}_1$ at $B_z = -0.86$ T and $\mathbb{S}_1$ at $B_z = 1.6$ T) are pinpointed, where $\mathrm{CD}_{\mathrm{ext}} = 0$ and $\mathrm{CD}_{\mathrm{sca}} = 0$, respectively. (f) The dependence of cross sections ($\mathrm{CD}_{\mathrm{ext}}$ at $\mathbb{E}_1$ and $\mathrm{CD}_{\mathrm{sca}}$ at $\mathbb{S}_1$) on the varying incident polarizations transversing half the great circle ($S_2 = 0$), covering LCP ($\theta = 0$), linear polarization along the x axis ($\theta = \pi/2$), and RCP ($\theta = \pi$).

can be expressed as (without extra interference terms)

$$C_{\mathrm{sca,ext}}(B_z) = \sin^2\left(\frac{\pi}{4}-\frac{\chi_i}{2}\right)C^{\circlearrowright}_{\mathrm{sca,ext}}(B_z) + \cos^2\left(\frac{\pi}{4}-\frac{\chi_i}{2}\right)C^{\circlearrowleft}_{\mathrm{sca,ext}}(B_z), \quad (2)$$

where $C^{\circlearrowright}_{\mathrm{sca,ext}}$ ($C^{\circlearrowleft}_{\mathrm{sca,ext}}$) are cross sections (scattering and extinction as indicated by the subscripts) for unit-amplitude incident RCP (LCP) wave; B_z is the externally applied magnetic field to magnetize the magneto-optical scatterers. It is clear from Eq. (2) that the scattering and extinction cross sections (i) are irrelevant to the orientations of the polarization ellipses (ψ_i independent) and thus are invariant for polarizations locating on the same latitude line of the Poincaré sphere, and (ii) for incident waves of arbitrary polarizations are ellipticity-weighted arithmetic average of those with RCP and LCP incidences, and they always reach their extremes for CP incident waves.

Simple algebraic manipulations reduce Eq. (2) to

$$C_{\mathrm{sca,ext}}(B_z) = \tfrac{1}{2}[C^{\circlearrowright}_{\mathrm{sca,ext}}(B_z) + C^{\circlearrowleft}_{\mathrm{sca,ext}}(B_z)] - \tfrac{1}{2}\sin(\chi_i)[C^{\circlearrowright}_{\mathrm{sca,ext}}(B_z) - C^{\circlearrowleft}_{\mathrm{sca,ext}}(B_z)]. \quad (3)$$

We further define the mean cross section for CP waves as $C^{+}_{\mathrm{sca,ext}}(B_z) = \frac{1}{2}[C^{\circlearrowright}_{\mathrm{sca,ext}}(B_z) + C^{\circlearrowleft}_{\mathrm{sca,ext}}(B_z)]$ and the cross section contrast as $C^{-}_{\mathrm{sca,ext}}(B_z) = \frac{1}{2}[C^{\circlearrowright}_{\mathrm{sca,ext}}(B_z) - C^{\circlearrowleft}_{\mathrm{sca,ext}}(B_z)]$. It is clear that $C^{+}_{\mathrm{sca,ext}}(B_z)$ represents exactly the cross sections for linearly polarized incident waves with $\chi_i = 0$. Then, Eq. (3) is further simplified as

$$C_{\mathrm{sca,ext}}(B_z) = C^{+}_{\mathrm{sca,ext}}(B_z) - \sin(\chi_i)C^{-}_{\mathrm{sca,ext}}(B_z). \quad (4)$$

The chiroptical responses of the scattering system can be characterized by a generalized chirality factor defined as [17]

$$\mathrm{CD}_{\mathrm{sca,ext}}(B_z) = 2\frac{C^{\circlearrowright}_{\mathrm{sca,ext}}(B_z) - C^{\circlearrowleft}_{\mathrm{sca,ext}}(B_z)}{C^{\circlearrowright}_{\mathrm{sca,ext}}(B_z) + C^{\circlearrowleft}_{\mathrm{sca,ext}}(B_z)} = 2\frac{C^{-}_{\mathrm{sca,ext}}(B_z)}{C^{+}_{\mathrm{sca,ext}}(B_z)}, \quad (5)$$

with which Eq. (4) becomes

$$C_{\mathrm{sca,ext}}(B_z) = C^{+}_{\mathrm{sca,ext}}(B_z)\left[1 - \tfrac{1}{2}\sin(\chi_i)\mathrm{CD}_{\mathrm{sca,ext}}(B_z)\right]. \quad (6)$$

When the chiroptical responses are eliminated $[\mathrm{CD}_{\mathrm{sca,ext}}(B_z) = 0]$, we have

$$C_{\mathrm{sca,ext}}(B_z) = C^{+}_{\mathrm{sca,ext}}(B_z), \quad (7)$$

which means that the scattering or extinction cross sections become fully independent of the incident polarizations.

III. SCATTERING PROPERTIES AND CHIROPTICAL RESPONSES OF ROTATIONALLY SYMMETRIC MAGNETO-OPTICAL SCATTERERS

Our model and formalisms presented in Sec. II are generally applicable to any configuration exhibiting no less than threefold rotation symmetry. As a next step, without loss of generality, we turn to a specific threefold rotationally symmetric scattering configuration shown in Fig. 1(b) for verifications of our model. It consists of two sets of three identical magneto-optical circular cylinders (for larger cylinders: radius $r_0 = 8$ μm and height $h_0 = 120$ μm; for smaller ones: $r_0 = 5$ μm and $h_0 = 60$ μm) and they are centered on vertices of equilateral triangles with all axes of the cylinders orientated along the z axis. The cylinders are made of magneto-optical materials, and the relative permittivity tensor $\overline{\overline{\varepsilon}}$ can be expressed as ($\perp$ denotes the components on the transverse x-y plane)

$$\overline{\overline{\varepsilon}} = \begin{bmatrix} \varepsilon_\perp & -i\varepsilon_B & 0 \\ i\varepsilon_B & \varepsilon_\perp & 0 \\ 0 & 0 & \varepsilon_z \end{bmatrix}. \quad (8)$$

For the magneto-optical polar semiconductor material n-doped InSb, the entries in the matrix above can be expressed as (adopting the Drude-like model and neglecting the higher-order magnetic terms) [18,19]

$$\varepsilon_\perp/\varepsilon_\infty = \frac{\omega_L^2 - \omega^2 - i\Gamma_p\omega}{\omega_T^2 - \omega^2 - i\Gamma_p\omega} + \frac{\omega_p^2(\omega + i\Gamma_f)}{\omega\left[\omega_c^2 - (\omega + i\Gamma_f)^2\right]};$$
$$\varepsilon_B/\varepsilon_\infty = \frac{\omega_p^2\omega_c}{\omega\left[(\omega + i\Gamma_f)^2 - \omega_c^2\right]};$$
$$\varepsilon_z/\varepsilon_\infty = \frac{\omega_L^2 - \omega^2 - i\Gamma_p\omega}{\omega_T^2 - \omega^2 - i\Gamma_p\omega} - \frac{\omega_p^2}{\omega(\omega + i\Gamma_f)}. \quad (9)$$

Here, ω is the angular frequency of the incident wave; $\varepsilon_\infty = 15.7$ is the high-frequency dielectric constant; $\omega_L = 2.28 \times 10^{14}$ rad/s is the longitudinal optical phonon frequency; $\omega_T = 2.13 \times 10^{14}$ rad/s is the transverse optical phonon frequency; $\omega_p = 1.97 \times 10^{14}$ rad/s is the plasma frequency; $\Gamma_p = 3.55 \times 10^{12}$ rad/s is the phonon damping constant; $\Gamma_f = 2.13 \times 10^{13}$ rad/s is the free carrier damping constant. The nondiagonal element ε_B is proportional to the cyclotron frequency $\omega_c = eB_z/m^*$, where e and m_0 are, respectively, the electron charge and mass, and the effective mass $m^* = 0.022\, m_0$.

Numerical results in this work are obtained through commercial software COMSOL MULTIPHYSICS. The simulation domain consists of six cylinders with the vacuum background truncated by perfectly matched layers (PMLs). The calculation domains can be automatically meshed according to the internal COMSOL MULTIPHYSICS algorithm, and further manual modifications of the mesh density can ensure computational convergence and sufficiently high data precision. For plane waves incident along the z axis, we show in Figs. 2(a)–(d) the scattering and extinction spectra for polarizations of the same [Figs. 2(a) and 2(c)] and different [Figs. 2(b) and 2(d)] latitude lines of the Poincaré sphere. It is clear that for both scenarios of zero [Figs. 2(a) and 2(b)] and nonzero [Figs. 2(c) and 2(d); $B_z = 1$ T] external magnetic field, the scattering and extinction cross sections are correlated with ellipticities only, and have nothing to do with the polarization ellipse orientations. We then randomly select an incident wavelength $\lambda_i = 210$ μm, and show at this wavelength the relation between $\mathrm{CD}_{\mathrm{sca,ext}}$ and B_z in Fig. 2(e). It is clearly shown that the chiroptical responses can be suppressed or enhanced, depending on the direction and strength of the magnetization. It is worth noting that the dependence of $\mathrm{CD}_{\mathrm{ext}}$ is more complicated than

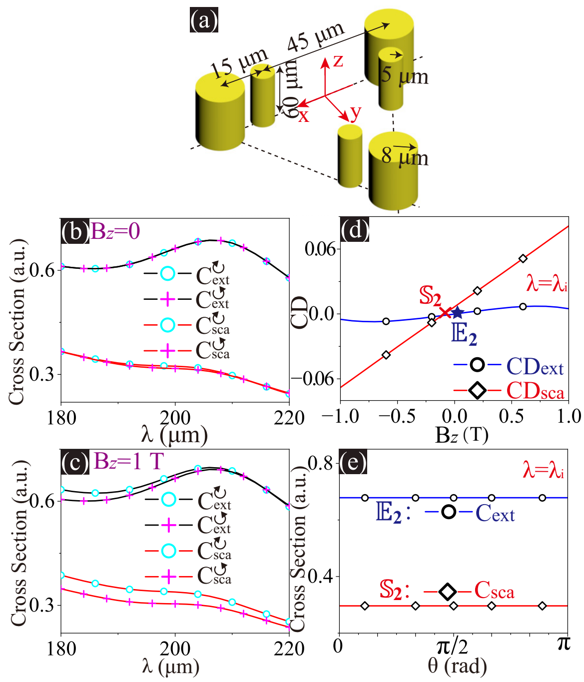

FIG. 3. (a) A modified scattering configuration that exhibits not only C_3 rotation symmetry, but also an extra mirror symmetry with the symmetry plane perpendicular to the z axis. Scattering and extinction spectra for incident RCP and LCP waves, with zero [$B_z = 0$ in (b)] and nonzero [$B_z = 1$ T in (c)] magnetizations. (d) The dependence of $CD_{sca,ext}$ on B_z at the incident wavelength $\lambda_i = 210$ μm. Two points ($\mathbb{E}_2$ at $B_z = 0$ and $\mathbb{S}_2$ at $B_z = -0.1$ T) are pinpointed, where $CD_{ext} = 0$ and $CD_{sca} = 0$, respectively. (e) The dependence of of cross sections (CD_{ext} at $\mathbb{E}_2$ and CD_{sca} at $\mathbb{S}_2$) on varying incident polarizations transversing half the great circle ($S_2 = 0$).

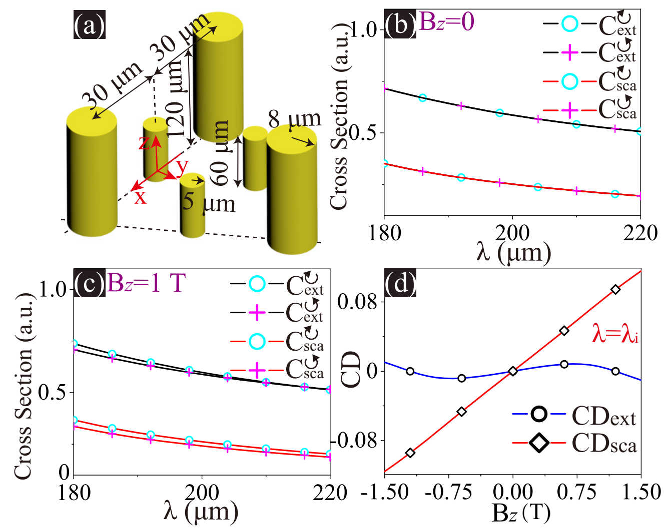

FIG. 4. (a) Another modified scattering configuration that exhibits not only C_3 rotation symmetry but also extra mirror symmetries with the symmetry planes parallel to the z axis. Scattering and extinction spectra for incident RCP and LCP waves, with zero [$B_z = 0$ in (b)] and nonzero [$B_z = 1$ T in (c)] magnetizations. (d) The dependence of $CD_{sca,ext}$ on B_z at the incident wavelength $\lambda_i = 210$ μm.

that of CD_{sca}, as is evident in Fig. 2(e). This is largely due to the sophisticated correlation between material absorption and B_z [Eq. (9)], since extinction is the sum of scattering and absorption according to the optical theorem [17].

We have further marked two points ($\mathbb{E}_1$ at $B_z = -0.86$ T and $\mathbb{S}_1$ at $B_z = 1.6$ T) where the chiroptical responses in terms of extinction and scattering cross sections are completely eliminated, respectively ($CD_{ext,sca} = 0$). At those points, we show in Fig. 2(f) the evolutions of the corresponding cross sections (CD_{ext} at $\mathbb{E}_1$ and CD_{sca} at $\mathbb{S}_1$) for varying incident polarizations covering the semigreat circle of $S_2 = 0$ ($\theta = 0$ for LCP; $\theta = \pi/2$ for linear polarization along the x axis; $\theta = \pi$ for RCP). As expected [see Eq. (7)], both extinction and scattering cross sections remain invariant, and are fully independent of polarization states of incident waves.

It has been previously proved that for reciprocal structures, combined rotation and mirror (perpendicular to the rotation axis) symmetries would eliminate the chiroptical response in terms of extinctions ($CD_{ext} = 0$), and thus render the extinction cross sections fully independent of the incident polarization [6,7]. The configuration shown in Fig. 1(b) is modified to a new configuration shown in Fig. 3(a) that exhibits both C_3 rotation symmetry and a perpendicular mirror symmetry. We further show in Fig. 3(b) ($B_z = 0$) and Fig. 3(c) ($B_z = 1$ T) the scattering and extinction spectra with incident CP waves for the modified scattering cluster. The dependence of $CD_{sca,ext}$ on B_z at $\lambda_i = 210$ μm is summarized in Fig. 3(d), where two other chiroptical response elimination points are marked ($\mathbb{E}_2$ at $B_z = 0$ on which $CD_{ext} = 0$, and $\mathbb{S}_2$ at $B_z = -0.1$ T, on which $CD_{sca} = 0$). The incident polarization independence of the corresponding cross sections at $\mathbb{E}_2$ and $\mathbb{S}_2$ are further confirmed by Fig. 3(e). The symmetry-reciprocity-induced elimination of chiroptical response CD_{ext} is confirmed by Figs. 3(b) and 3(d) [see $\mathbb{E}_2$]. When the scatterer is magnetized ($B_z \neq 0$), reciprocity is broken and thus the chiroptical responses in terms of extinction would generally be restored [Fig. 3(d)].

It has also been proved that joint operations of rotation and mirror (parallel to the rotation axis) symmetries would eliminate chiroptical responses in terms of not only extinction ($CD_{ext} = 0$) but also scattering ($CD_{sca} = 0$), and make all cross sections polarization independent. We have studied such a structure shown in Fig. 4(a), with the polarization independence of scattering and extinction cross sections confirmed by Fig. 4(b). With the presence of external magnetic field ($B_z \neq 0$), magnetization would effectively break the mirror symmetries, and thus render both cross sections dependent on the incident polarizations gain, as verified by the spectra shown in Fig. 4(c) with $B_z = 1$ T. The dependence of $CD_{sca,ext}$ on B_z at $\lambda_i = 210$ μm for this scattering configuration is shown in Fig. 4(d), which further confirms that external magnetizations restore the chiroptical responses and polarization dependence of both scattering and extinction cross sections.

IV. CONCLUSION AND PERSPECTIVE

To conclude, we study the interplay between geometric structural chiralities and external magnetizations, and explore how their competitions affect the chiroptical responses of scattering systems. It is revealed that for magneto-optical scatterers, an externally applied static magnetic field can suppress or enhance the chiroptical responses, depending on the direction and strength of the magnetizations. With properly designed magnetic field, the optical chiralities in terms of scattering and extinction cross sections can be fully eliminated, which together with the rotation symmetry would induce scattering properties that are fully independent of arbitrary incident polarizations. All our conclusions drawn are based on principles of symmetries and thus are broadly applicable, which are protected by global structural symmetries and are irrelevant to detailed geometric shapes or optical material parameters. The principles we have revealed might find significant applications in various branches of photonics that involve magnetism and particle scattering.

In this study, we have explored the overlapped regions among various disciplines of Mie scattering, chiral optics, geometric symmetries in optics, and electromagnetic nonreciprocity. Possible future works and extensions include incorporating other symmetries (such as electromagnetic duality symmetry [8,9] and parity-time symmetry [20,21]), merging with synthetic magnetism and other synthetic dimensions in photonics [22,23], and introducing temporal modulations and the exceptional concept of time crystals [24,25]. Those potential extensions and generalizations can not only significantly broaden the horizons of all disciplines involved, but also bring extra dimensions of freedom to exploit for extreme light-matter interaction manipulations.

ACKNOWLEDGMENTS

This research was funded by the National Natural Science Foundation of China (Grants No. 12274462, No. 11674396, and No. 11874426) and several other projects of Hunan Province (Projects No. 2024JJ2056, No. 2023JJ10051, No. 2018JJ1033, and No. 2017RS3039).

[1] L. D. Barron, *Molecular Light Scattering and Optical Activity* (Cambridge University Press, Cambridge, 2009).

[2] *Singular and Chiral Nanoplasmonics*, 1st ed., edited by S. Boriskina and N. I. Zheludev (Jenny Stanford Publishing, Singapore, 2014).

[3] J. T. Collins, C. Kuppe, D. C. Hooper, C. Sibilia, M. Centini, and V. K. Valev, Chirality and chiroptical effects in metal nanostructures: Fundamentals and current trends, Adv. Opt. Mater. **5**, 1700182 (2017).

[4] J. Mun, M. Kim, Y. Yang, T. Badloe, J. Ni, Y. Chen, C.-W. Qiu, and J. Rho, Electromagnetic chirality: From fundamentals to nontraditional chiroptical phenomena, Light: Sci. Appl. **9**, 139 (2020).

[5] W. Chen, Q. Yang, Y. Chen, and W. Liu, Extremize optical chiralities through polarization singularities, Phys. Rev. Lett. **126**, 253901 (2021).

[6] W. Chen, Q. Yang, Y. Chen, and W. Liu, Scattering activities bounded by reciprocity and parity conservation, Phys. Rev. Res. **2**, 013277 (2020).

[7] Q. Yang, W. Chen, Y. Chen, and W. Liu, Symmetry protected invariant scattering properties for incident plane waves of arbitrary polarizations, Laser Photonics Rev. **15**, 2000496 (2021).

[8] I. Fernandez-Corbaton, X. Zambrana-Puyalto, N. Tischler, X. Vidal, M. L. Juan, and G. Molina-Terriza, Electromagnetic duality symmetry and helicity conservation for the macroscopic Maxwell's equations, Phys. Rev. Lett. **111**, 060401 (2013).

[9] Q. Yang, W. Chen, Y. Chen, and W. Liu, Electromagnetic duality protected scattering properties of nonmagnetic particles, ACS Photonics **7**, 1830 (2020).

[10] A. I. Kuznetsov, A. E. Miroshnichenko, M. L. Brongersma, Y. S. Kivshar, and B. Luk'yanchuk, Optically resonant dielectric nanostructures, Science **354**, aag2472 (2016).

[11] W. Liu and Y. S. Kivshar, Generalized Kerker effects in nanophotonics and meta-optics, Opt. Express **26**, 13085 (2018).

[12] J. Qin, S. Xia, W. Yang, H. Wang, W. Yan, Y. Yang, Z. Wei, W. Liu, Y. Luo, L. Deng, and L. Bi, Nanophotonic devices based on magneto-optical materials: Recent developments and applications, Nanophotonics **11**, 2639 (2022).

[13] A. Yariv and P. Yeh, *Photonics: Optical Electronics in Modern Communications*, 6th ed. (Oxford University Press, New York, 2006).

[14] S. Ramaseshan, The Poincaré sphere and the Pancharatnam phase: Some historical remarks, Curr. Sci. **59**, 1154 (1990).

[15] E. Cartan, *The Theory of Spinors* (Courier Corporation, Chelmsford, 2012).

[16] G. Farmelo, *The Strangest Man: The Hidden Life of Paul Dirac, Mystic of the Atom* (Basic Books, New York, 2011).

[17] C. F. Bohren and D. R. Huffman, *Absorption and Scattering of Light by Small Particles* (Wiley, New York, 1983).

[18] E. D. Palik, R. Kaplan, R. W. Gammon, H. Kaplan, R. F. Wallis, and J. J. Quinn, Coupled surface magnetoplasmon-optic-phonon polariton modes on InSb, Phys. Rev. B **13**, 2497 (1976).

[19] E. Moncada-Villa, V. Fernández-Hurtado, F. J. García-Vidal, A. García-Martín, and J. C. Cuevas, Magnetic field control of near-field radiative heat transfer and the realization of highly tunable hyperbolic thermal emitters, Phys. Rev. B **92**, 125418 (2015).

[20] R. El-Ganainy, K. G. Makris, M. Khajavikhan, Z. H. Musslimani, S. Rotter, and D. N. Christodoulides, Non-Hermitian physics and PT symmetry, Nat. Phys. **14**, 11 (2018).

[21] Ş. K. Özdemir, S. Rotter, F. Nori, and L. Yang, Parity–time symmetry and exceptional points in photonics, Nat. Mater. **18**, 783 (2019).

[22] L. Yuan, Q. Lin, M. Xiao, and S. Fan, Synthetic dimension in photonics, Optica **5**, 1396 (2018).

[23] E. Lustig and M. Segev, Topological photonics in synthetic dimensions, Adv. Opt. Photonics **13**, 426 (2021).

[24] S. Saha, O. Segal, C. Fruhling, E. Lustig, M. Segev, A. Boltasseva, and V. M. Shalaev, Photonic time crystals: A materials perspective, Opt. Express **31**, 8267 (2023).

[25] M. P. Zaletel, M. Lukin, C. Monroe, C. Nayak, F. Wilczek, and N. Y. Yao, *Colloquium*: Quantum and classical discrete time crystals, Rev. Mod. Phys. **95**, 031001 (2023).